Adsorption of Indium on a InAs wetting layer deposited on the GaAs(001) surface

Marcello Rosini* and Rita Magri

Dipartimento di Fisica dell'universitá degli studi di Modena e Reggio Emilia and S3 research center of CNR-INFM, via Campi 213/A, 41100 Modena, Italy

Peter Kratzer

Fachbereich Physik, Universität Duisburg-Essen, Germany

(Dated: February 5, 2008)

Abstract

In this work we perform a first-principles study of the adsorption properties of an In adatom deposited on 1.75 monolayers (ML) InAs, forming a wetting layer on GaAs(001) with the $\alpha_2(2\times4)$ or $\beta_2(2\times4)$ reconstruction. The structural properties of these reconstructions have been studied: we determine the equilibrium geometry of the surfaces and their stability for various growth conditions. We have then carried out a detailed study of the potential energy surface (PES) for an In adsorbate, finding the minima and the saddle points. The main characteristics of the PES and the bonding configurations of the In adatom on the surface are analyzed by comparing with analogous studies reported in the literature, trying to extract the effects due to: (i) the compressive strain to which the InAs adlayer is subjected, (ii) the particular surface reconstruction, and (iii) the wetting layer composition. We found that, in general, stable adsorption sites are located at: (i) locations besides the As in-dimers, (ii) positions bridging two As in-dimers, (iii) between two adjacent ad-dimers (only in β_2), and (iv) locations bridging two As ad-dimers. We find also other shallower adsorption sites which are more reconstruction specific due to the lower symmetry of the α_2 reconstruction compared to the β_2 reconstruction.

PACS numbers: 68.43.Jk, 31.50.-x

*Electronic address: mrosini@unimo.it

I. INTRODUCTION

Thanks to the strong charge carrier confinement, QDs have atomic-like properties that could be useful for applications in optical and optoelectronic devices, quantum computing, and information storage. One of the most challenging problems for quantum dot formation, is the control of their shape, composition and density. From this point of view the abundant experimental knowledge has not yet produced a sufficiently deep understanding of the physics of formation of quantum dots that could guide the way to control the growth process. In this situation first-principles simulations can be helpful in sheding light on the atomistic mechanisms that lead to dot nucleation at surfaces.

In the present paper, we address one of the most-studied systems: InAs quantum dots grown on a GaAs(001) substrate, where the lattice mismatch between InAs and GaAs is of the order of 7%. Strain relaxation at the surface acts as a driving force for a self-assembly process, the so called Stranski-Krastanov growth mode [1], with the deposition of an atomically thin InGaAs wetting layer (WL) and subsequent surface mass transport accompanied by a 2D to 3D growth transition.

We focus our attention on the structural properties of the WL on which quantum dots nucleate, and on the interaction between a single In adatom and the surface, in order to find where the diffusion barriers are located and what the possible adsorption sites on the surface are, as a function of the wetting layer reconstruction.

We have chosen to investigate mainly the $\alpha_2(2 \times 4)$ reconstruction of the (001) surface because of its stability under In-rich conditions and under compressive strain [2, 3, 4] which is the case for the InAs WL grown on GaAs. Moreover, a (2×4) reconstruction was found [5, 6, 7, 8] to occur on the (001) wetting layer at the onset of dot nucleation in a In-rich WL condition. We have modeled a WL at a InAs coverage $\theta = 1.75$ monolayer (ML) which is close to the critical value corresponding to the 2D to 3D transition [9]. The structural and geometrical properties of this surface have been investigated. Using the α_2 reconstruction we have calculated the PES for a single In adatom, with the aim to understand what are the implications of the WL morphology (strain and composition) on the adsorption and surface mobility of the deposited In. To this end a comprehensive comparison with results reported previously in the literature for Ga and In adatoms and other surface reconstructions is given. In this context, a detailed analysis of the differences and analogies between the α_2 and the

β_2 reconstructions is pursued.

In the literature similar calculations have been reported for GaAs [100] homoepitaxy [10]. The issue of the WL composition for In adsorption has been addressed only by Penev et. al. [11, 12], but for a much lower In coverage of $\theta = 0.66$ ML.

The paper is organized as follows: in section II we detail our theoretical approach. Section III reports the obtained results for: (i) the WL surface reconstruction and energy; (ii) the PES of a single In adatom on the α_2 and the β_2 reconstructed WL; (iii) the determination of the barrier positions and heights between each couple of adsorption sites; (iv) a detailed study of the atomic bonding of the In adatom to the WL. In section IV our results are compared with those regarding other surface reconstructions in order to extract a rationale for the dependence on In adsorption and diffusion on the local structure of the (001) surface. Finally, a summary is given at the end of the paper.

II. THEORETICAL METHOD

We performed first principles calculations within Density Functional Theory in the local density approximation (DFT-LDA) [13] using the exchange and correlation potential of Ceperley and Alder [14] as parametrized by Perdew and Zunger [15]. For this kind of calculations both LDA [2, 16, 17, 18, 19] and GGA [10, 12, 20, 21, 22] have been used in the literature. It has been demonstrated [23, 24] that both methods give qualitatively the same picture for the description of adatom adsorption on a surface, although LDA usually gives larger values for binding energies than GGA [25]. Only the details can be different: LDA tends to overestimate the binding energy but for lattice constants, elastic moduli and surface energies the LDA calculated values are generally closer to the experimentally determined ones. We have used norm-conserving pseudopotentials treating the outermost s- and p-shells of Ga, In and As as valence electrons, and the electronic wave functions were expanded in plane-waves, with a 18 Ry kinetic energy cutoff. The energy cutoff has been tested in order to reach convergence for the lattice bulk properties of GaAs and InAs. The core corrected atomic pseudopotentials have been tested on bulk Ga, In and As, where the determined equilibrium configurations and elastic moduli compare well with the experimental data.

The equilibrium lattice parameters obtained for the GaAs and InAs bulk phases are $a_0 = 5.609$ Å and $a_0 = 5.906$ Å, which are slightly smaller than the experimental ones.

Thus our calculated lattice mismatch is 5.4%, smaller than the experimental value. This is going to underestimate the WL strain. In sec. IV we will compare our results with results [10, 12, 16] where this effect was instead overestimated.

Starting from the GaAs structure, we have set up the (001) oriented supercell containing 4 layers of GaAs, covered with 1.75 layers of InAs arranged according to the $\alpha_2(2\times4)$ surface reconstruction. The lower layer of Ga atoms is kept fixed during the cell relaxation, in order to mimic the constraint due to the underlying semi-infinite bulk, and it is passivated with pseudo hydrogen atoms of 1.25 electron charge. The slab is repeated along the (001) direction with a periodicity $5a_0$ and a separation of about 10 Å of vacuum. As for the number of GaAs layers, we have found that only two layers suffice to obtain a correct description of the PES, minima and maxima positions. The refinement using two more GaAs layers produces a difference in the barrier heights all within 40 meV. Brillouin-zone (BZ) integration was carried out using a set of special k-points equivalent to 16 points in the 1×1 surface BZ. A smearing of 0.02 Ry has been used in order to account for the possible metalization of the surface electronic structure.

In the $\alpha_2(2\times4)$ reconstruction the last complete atomic layer is constituted by As atoms. A $\theta = 0.75$ cation layer is deposited over it. This layer is then terminated with one As dimer (As ad-dimer) on top (see Fig. 1). The uncovered As on the last complete layer dimerizes along the $[\bar{1}10]$ direction (As in-dimer). The $\beta_2(2\times4)$ reconstruction is similar but presents one additional As ad-dimer bridging the two remaining In rows on the top of the surface (see Fig. 1). It has a larger symmetry than the α_2 reconstruction, being mirror symmetric with respect to the (110) plane passing through the As in-dimers. All the examined structures have been relaxed in order to find the equilibrium geometries, until all the forces acting on the atoms were less than $2.5\cdot10^{-3}$ eV/Å.

The PES of an In adatom is calculated by relaxing the adatom z component together with all the surface degrees of freedom while the in-plane x, y coordinates are kept fixed. We have set up a grid of 8×4 points, corresponding to a step of 2 Å, along the (110) and $(\bar{1}10)$ directions respectively, and for each point we have found the minimum energy configuration for the adsorbate plus surface. Then we have interpolated the grid data with a bi-cubic spline algorithm in order to find the positions of the minima and the saddle points. The exact values of the minima have then been determined by further relaxing all the three coordinates of the adatom together with the surface. To minimize the adsorbate interaction

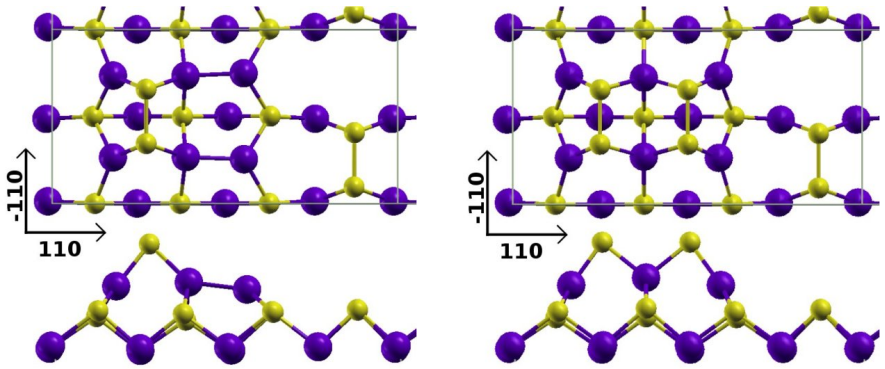

FIG. 1: (Color online) Representation of the $\alpha_2(2\times4)$ (left) and $\beta_2(2\times4)$ (right) surface reconstructions. The shown geometries are those optimized. It is evident the bending of the the In-In bond in the top layer in the α_2 reconstruction. Dark balls and light balls represent In and As ions respectively.

we have doubled the surface unit cell along the $(\bar{1}10)$ direction.

Since one of the objectives of this work is ultimately to study In diffusion on the WL within the framework of the Transition State Theory [26, 27, 28], the minimum energy paths (MEP) and the height of each energy barrier between every couple of adsorption sites have to be calculated, leading to a more detailed knowledge of the PES. This task has been accomplished by using the Nudged Elastic Band method (NEB). This method is able to find the MEP between two adsorption sites, by simulating a string of replicas of the system, where the different images are one linked to the other by springs [29, 30]. By minimizing the energy associated to the path, an accurate description of the MEP and thus of the saddle point is obtained.

All the ab-initio calculations were performed using the ESPRESSO simulation package [31].

III. RESULTS

A. Structure of $(001)(2\times4)$ surface reconstructions

We have calculated the optimized geometries and the formation energies of the $\alpha_2(2\times4)$ and $\beta_2(2\times4)$ reconstructions of the bare GaAs surface and of GaAs covered with a $\theta = 1.75$ ML InAs layer. The surface energies vs. the As chemical potential μ_{As} (whose value is

related to the growth conditions such as growth temperature, cation/anion flux ratios) are calculated through the expression [32]

$$\gamma_{\rm f} = \frac{1}{A}\left(E_{\rm tot} - N_{\rm Ga}\mu_{\rm GaAs} - N_{\rm In}\mu_{\rm InAs}\right) - \mu_{\rm As}\frac{N_{\rm As} - N_{\rm Ga} - N_{\rm In}}{A}\ , \qquad (1)$$

($\mu_{\rm InAs} = 0$, $N_{\rm In} = 0$ for pure GaAs). The obtained surface energies are reported in Fig. 2. Here $E_{\rm tot}$ is the total energy of the slab, $\mu_{\rm xx}$ is the chemical potential of the bulk phase of material xx, $N_{\rm y}$ is the number of atoms of element y in the supercell and A is the surface unit cell area. A set of calculations is performed for a slab with two hydrogen passivated surfaces, in order to subtract the contribution of the bottom surfaces of the reconstructed slabs to be investigated, hence $E_{\rm tot}$ is the net contribution of the reconstructed slab. Elemental As, Ga and In are calculated using their ground state structures: respectively the rhombohedral A7 structure for As, α-Ga and bct In. All these calculations have been done using high convergence standards. We see that the range of stability of the α_2 phase, when GaAs is covered with the InAs ad-layer, is larger than that of the bare GaAs surface. This means that the formation of the α_2 phase will be favored over the β_2 phase over a larger range of As flux values (or surface growth conditions), when the InAs WL is formed. This is in agreement with previous calculations showing a stabilization of the α_2 phase for InAs under isotropic compressive strain [2, 11] which is the condition of the InAs layer grown on GaAs.

Regarding the atomic structures, the comparison of the distances between the atomic planes, in the InAs covered GaAs case, shows that the values are systematically larger than those obtained for the pure GaAs surface by about 10 %, owing to the stress originated by the InAs/GaAs lattice mismatch. In particular, we remark the buckling of the bond between the In atoms in the uncompleted In layer found for the α_2 reconstruction (see Fig. 1) due to the missing (with respect to the β_2 reconstruction) second As ad-dimer. It was shown ([2]) that this buckling plays a role in the stabilization of the α_2 phase.

B. The potential energy surface of the single In adatom

In the following we describe our calculations for both the α_2 and β_2 surface reconstructions, with an accurate description of the adsorption sites and hopping barriers.

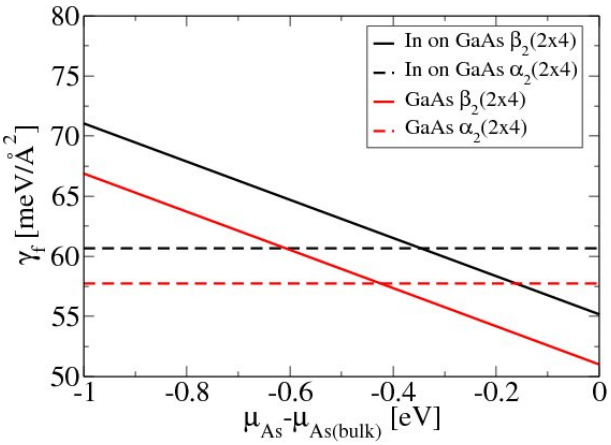

FIG. 2: (Color online) Surface energy phase diagram for the $\alpha_2(2\times4)$ and $\beta_2(2\times4)$ reconstructions of InAs/GaAs(001) and GaAs(001).

1. $\alpha_2(2\times4)$ *surface reconstruction*

For this surface reconstruction we have found eleven adsorption sites for the In adatom, and the related saddle points. The energies of the minima and of the saddle points are given in Tables I and II, respectively, and a graphical representation of the PES is reported in Fig. 3. In the Tables, the energies are relative to that of the deepest adsorption site A_8 put to 0. Two main low potential trenches are evident along the $[\bar{1}10]$ direction, at both sides of the As in-dimer row. The deepest adsorption site A_8 is located in the trench near the In vacancy of the surface layer and is bonded to the two As atoms of the in-dimer and to one In atom (see Fig. 4(a)). Other deep minima (A_4, A_6, and A_9) are located along the two deepest trenches and, together with A_8, represent the lowest energy set of minima. Their adsorption configuration is similar to that of A_8. A second class of adsorption sites (A_1, A_3, A_5, A_{11}) is characterized by the In adatom bonded to two other In atoms (see the configuration at minimum A_5 in Fig. 4(b)). At the minima A_7 and A_2 the adatom is bonded to four In atoms, reproducing the bonding scheme typical of bulk Indium (Fig. 4(c)). In these last cases the corresponding surface electronic structure is metallic. To the last class of adsorption sites belongs the shallow minimum A_{10} where the adatom is bonded to the two As of the ad-dimer (see Fig. 4(d)). This configuration plays the role of a precursor for the much stronger bonding of In into the ad-dimer (see below).

We have accurately checked that the shallow minima in the PES are actually minima and

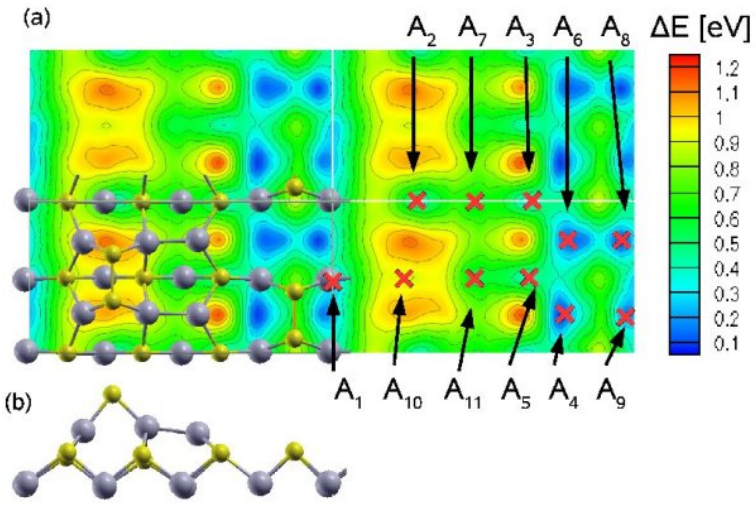

FIG. 3: (Color online) (a) PES of an In adatom on the α_2 (2×4) surface. The PES is drawn for 4 surface unit cells and a top view of the atomic structure is also shown. The minima are labeled A_i. (b) Side view of the surface layer.

not saddle points of the energy landscape.

The location of the calculated barriers T_n is shown in Fig. 5(a). The barriers are lower along the $[\bar{1}10]$ direction (the highest barrier being 430 meV and the lowest being 52 meV) than along the orthogonal [110] direction (see Table II). This difference is mainly ascribed to the presence of the As ad-dimer oriented along the $[\bar{1}10]$ direction, that creates an unstable region for the In adsorption, as can be seen in the PES of Fig 3. From these considerations we can preliminarily conclude that adatom surface diffusion should be strongly anisotropic with the $[\bar{1}10]$ direction along the trenches favored.

2. $\beta_2(2 \times 4)$ surface reconstruction

Since the symmetric part of the β_2 has the same structure of half of the α_2 surface, the coordinates of the adsorption sites can be roughly estimated, and their exact location can be found with a further relaxation of the surface-adsorbate system.

Also for the β_2 surface reconstruction, we have found 11 adsorption sites for the Indium adatom (see Table III and Fig. 5(b)). However, owing to the symmetry properties of the system, those minima reduce to only 6 inequivalent minima.

We first notice that the adsorption sites A_1, A_2, A_4, A_6, A_7, A_8, A_9, are in strict corre-

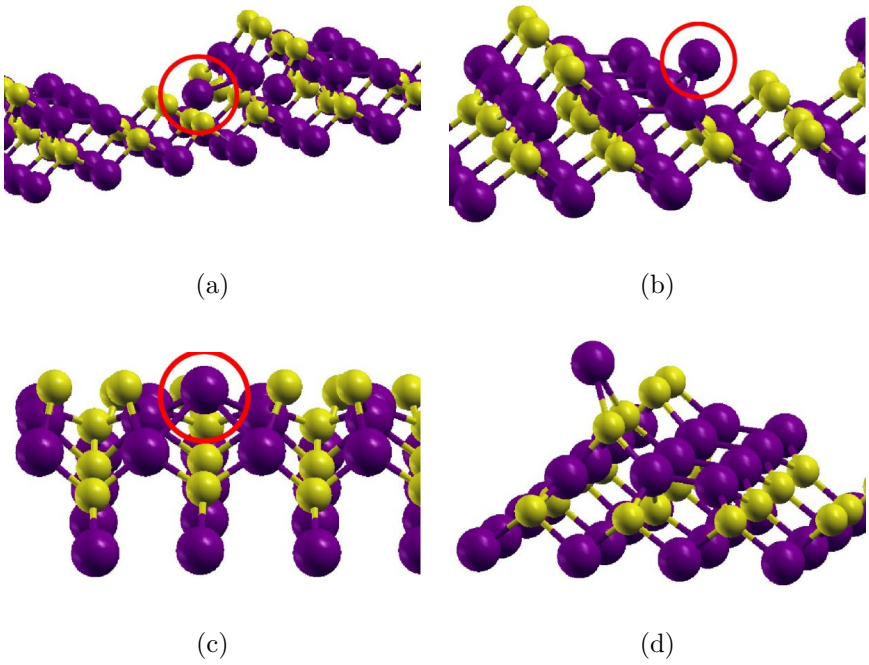

FIG. 4: (Color online) Adsorption configurations for the In adatom in different adsorption sites on the α_2 surface reconstruction. (a) Configuration A_8 (b) Configuration A_5 (c) Configuration A_2 (d) Configuration A_{10}

spondence to those of the α_2 surface reconstruction (see Fig 5), in the region where the two structures are similar i.e. far from the β_2 second ad-dimer. The positions of the minima are only slightly affected by the presence of the extra As ad-dimer, and the deepest adsorption site A_8 lies in the same position as for the α_2 reconstruction. The minima A_3 and A_5 are shifted towards the trench with respect to the corresponding ones of the α_2 reconstruction. This is due to the fact that the In adatoms in A_3 and A_5 on the α_2 reconstruction are bonded to the buckled In at the trench edge. The same In is not buckled in β_2 due to its bond to the second As ad-dimer row (compare Fig. 4(b) to Fig. 6(a)). To quantify the difference between the A_1-A_9 adsorption sites in the two reconstructions, we give in Table IV the adsorption energy difference $\Delta E = E^{\beta}(A_i) - E^{\alpha}(A_i)$ (negative if In is more strongly bonded in the β_2 than in α_2 reconstruction) and the displacement $\Delta r = \sqrt{\sum_i (r_i^{\beta} - r_i^{\alpha})}$ between the corresponding binding locations. The adsorption energy is defined as

$$E^{\alpha}(A_i) = E(\alpha_2 + \mathrm{In}_{A_i}) - E(\alpha_2) - E(\mathrm{In}) \ . \tag{2}$$

In β_2, $A_{3'}$ Fig 5 is the symmetric of the minimum A_3. This minimum is not present in the

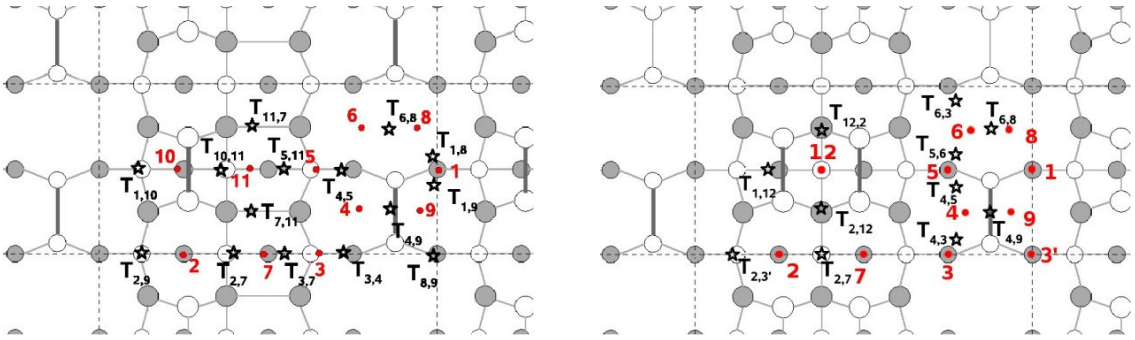

(a) (b)

FIG. 5: (Color online) Schematic view of the adsorption sites locations (only i is written) on the: (a) α_2 (2×4) and (b) β_2 (2×4) reconstructions. The saddle points are labeled as $T_{i,j}$.

α_2 reconstruction because of the lower symmetry. A new minimum A_{12} is now present for β_2 on top of the two ad-dimers and it is actually quite stable, since the In-adatom is fourfold bonded to the surface (see fig. 6(b)). In this case the confinement barriers are calculated to be of the order of 135 meV. The configuration for In in the adsorption sites different from those of the α_2 reconstruction, are given in Fig. 6.

Also in the β_2 case, two trenches in the PES are evident along the $(\bar{1}10)$ direction at both sides of the As in-dimer. The existence of the A_{12} adsorption site on β_2 could originate additional diffusion paths along the same direction connecting the minimum A_{12} to the two sites A_2 and A_7. The corresponding saddle point energies are reported in Table V. We can easily see that the barriers along $[\bar{1}10]$, are in the range 100-580 meV and are lower than the barriers along the [110] direction that span the range 100-760 meV. This consideration strongly indicates that also for the β_2 surface reconstruction, the In-adatom diffusion should be highly favored along the $(\bar{1}10)$ direction.

C. Additional adsorption sites due to In insertion in the As dimers

We know from the literature [16, 20] that additional minima could be present, corresponding to the In adatom breaking the bond between the As adatoms in a dimer and binding itself to them. This process requires overcoming an energy barrier, thus its rate should depend on the growth temperature. These sites can be of significant interest, since they introduce a local modification of the PES that can be very important for surface diffusion.

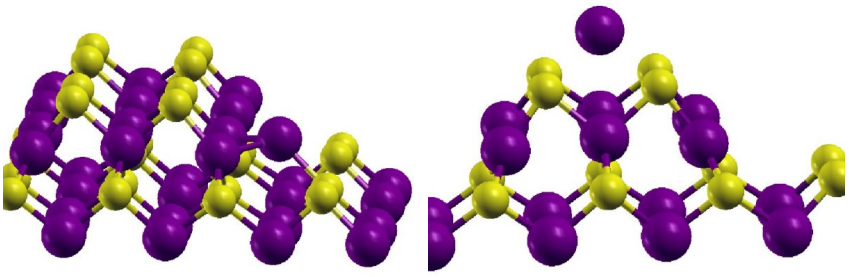

(a) (b)

FIG. 6: (Color online) Adsorptions configurations for the In adatom on the β_2 surface reconstruction. (a) Configuration A_5 (b) Configuration A_{11}

For example, such sites could be in a bridge location between two other adsorption sites, thus introducing a further minimum in an otherwise thicker barrier. Such an additional adsorption site can affect the diffusion kinetics of the In adatom on the surface.

We have considered both the As in-dimers and ad-dimers of the α_2 and β_2 surface reconstructions and determined the energy necessary to break the As-As bond and bind the In adatom. First of all we have put In in the middle between the two As atoms, in a vertical plane containing all the three atoms. We have then relaxed the system obtaining the minimum energy position for the In adatom. Finally we have performed different NEB calculations in order to find the energy barriers between these adsorption sites and the neighboring sites. We have found that the adsorption configuration with the In atom bonded to the two arsenic of the dimers are in general more stable than most of the other adsorption sites (see Tables I and III).

1. $\alpha_2(2 \times 4)$ surface reconstruction

In this case we have found 2 additional stable sites for the In adsorbate. The first one corresponds to the breaking of the As ad-dimer and the second one to the breaking of the As in-dimer. The two cases are shown in figures 7 and 8, respectively. Figures 7(a) and 8(a) show the location of these minima, indicated as A_a and A_i respectively, on the surface (a =ad-dimer i =in-dimer). Figures 7(b) and 8(b) show the atomic configuration of the adsorbate bonded to the As atoms in the dimers. The transitions to/from neighboring adsorption sites are also drawn in the figures (Figs. 7(c) and 8(c)) and the corresponding

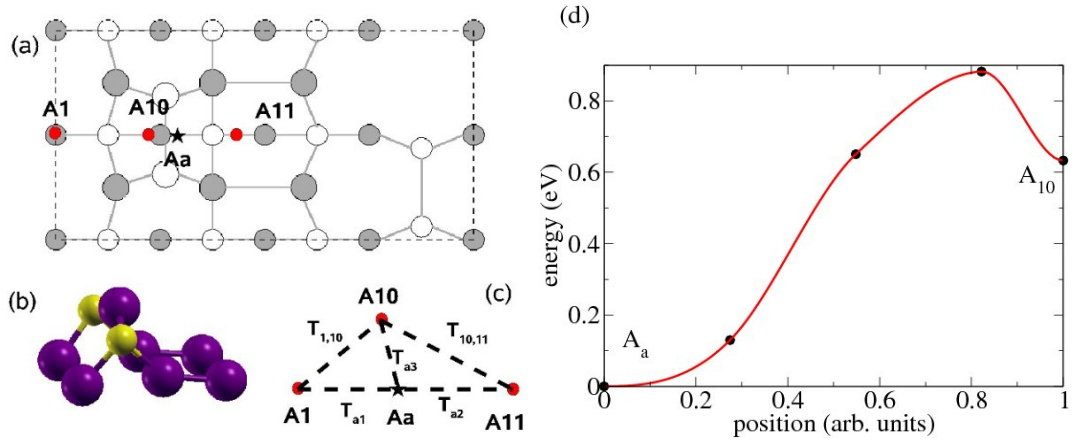

FIG. 7: (Color online) Additional adsorption site A_a due to the In insertion into the As ad-dimer on the α_2 reconstruction. (a) The location of the adsorption site is indicated by a star. (b) Atomic configuration. (c) Scheme of the transitions between the A_a adsorption site and the neighboring sites. (d) Energy profile for barrier T_{a3} from the precursor site A_{10} to A_a.

minima and saddle point energies are given in Tables I and II respectively. We can see that those minima are deep and stable, since the confining barriers ($\simeq$ 0.8 eV), pictured in Figures 7(d) and 8(d) are high. The energy barrier needed to fall into A_a from the site A_{10} (the precursor site) is not too high (around 200 meV) and this process is likely to occur even at relatively low temperature.

2. $\beta_2(2 \times 4)$ surface reconstruction

In this case we have two As ad-dimers instead of one. We have found one adsorption site for the In adatom for each one of the ad-dimers indicated in Figures 9 as A_{a1} and A_{a2}. We have found that the In adsorbate does not lie in the vertical plane passing through the As dimers, but the bonds are tilted towards the other ad-dimer, that is towards the symmetry plane passing through the A_{12} adsorption site. Regarding the As in-dimer we have found two distinct possibilities for In adsorption that we indicate as A_{i1} and A_{i2} in Figure 10. As can be seen from Fig. 10(b), the In atom bonds to the two As of the in-dimer forming a tilted angle ϕ with respect to the vertical z direction. Since the (110) is a plane of symmetry for the system, the two configurations for the adsorbate, corresponding to angles ϕ and $-\phi$, with respect to the z axis are equivalent and have the same probability to occur.

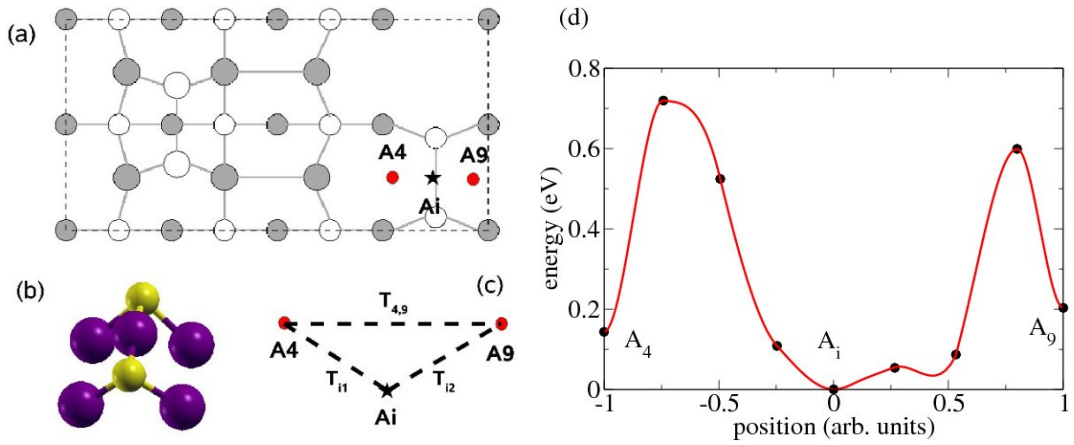

FIG. 8: (Color online) Additional adsorption site A_i due to the In insertion into the As in-dimer on the α_2 surface reconstruction. (a) The location of the adsorption site is indicated by a star. (c) Atomic configuration. (b) Scheme of the transitions between the A_i adsorption site and the neighboring sites. (d) Energy profile for barriers T_{i1} and T_{i2} from the two besides in-dimer adsorption sites A_4 and A_9 to A_i.

Figures 9(a) and 10(a) show the location of the adsorption sites for the As ad-dimers and As in-dimer, respectively. The atomic configurations for the adsorbates are given in Figures 9(b) and 10(b), whereas the transitions to/from neighboring adsorption sites are reported in Figures 9(c) and 10(c). Finally Figures 9(d) and 10(d) plot the energy barriers separating these adsorption sites from the neighboring ones.

Tables III and V report the energies for the stable configurations and the corresponding saddle points. Even in this case we have found very high binding energies for these adsorption sites and high energy barriers (around 0.7 eV) that make these configurations very stable once the adatom reaches them overcoming the barriers.

IV. DISCUSSION

In order to evaluate the effects of the strain and the role of the different surface reconstructions on the In adsorption properties we now compare our results with the results of similar calculations reported in the literature. To better evaluate the differences we report in Fig. 11 the more common adsorption features as extracted by the literature and the present work. In the same figure we name each specific adsorption site with respect to its position

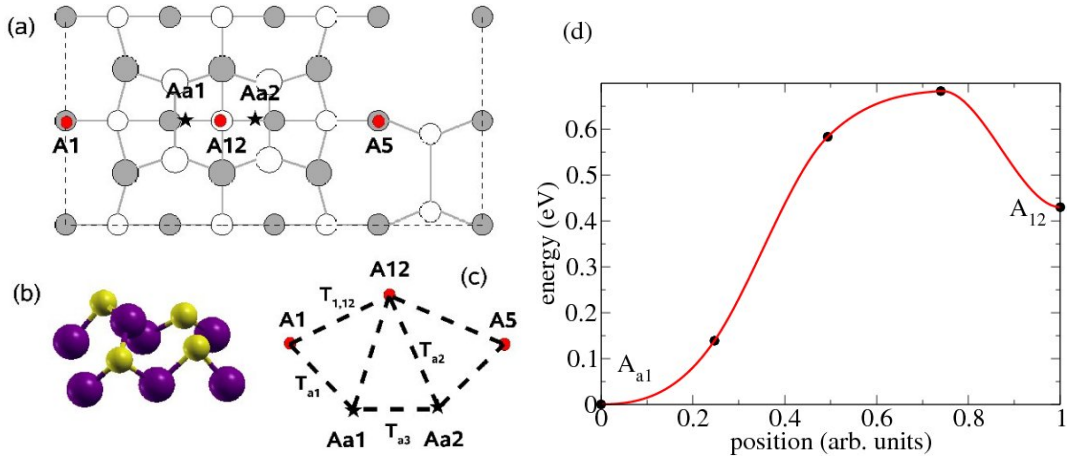

FIG. 9: (Color online) Additional adsorption sites A_{a1} and A_{a1} due to the In insertion into the As ad-dimer on the β_2 surface reconstruction. (a) The location of the adsorption sites are indicated by stars. (b) Atomic configuration. (c) Scheme of the transitions between the A_{a1} and A_{a1} adsorption site and the neighboring sites. (d) Energy profile for barriers T_{a2} from the top ad-dimer adsorption site A_{12} to A_a.

relative to the As in-dimers (i) and ad-dimers (a), and indicate also the reconstructions where these adsorption sites are typical.

A. α_2 vs β_2 reconstruction (this work)

There are no big differences between the adsorption features on the α_2 and on the β_2 surface reconstructions. In particular, the adsorption energy and location differences (see Table IV) between corresponding adsorption sites, are within a few hundreds of meV. The greatest differences are those in the region of the missing ad-dimer where the structural difference between the two surface reconstructions is larger. On the β_2 reconstruction the positions and energies of the adsorption sites are modified owing to the symmetry properties of the reconstruction. The most important difference is the presence of the adsorption sites $A_{3'}$ and A_{12} on the β_2 surface reconstruction, that are absent on the α_2 surface reconstruction. On the contrary, the adsorption sites A_{10} and A_{11} of α_2 disappear in β_2 transforming into the top ad-dimer site A_{12}.

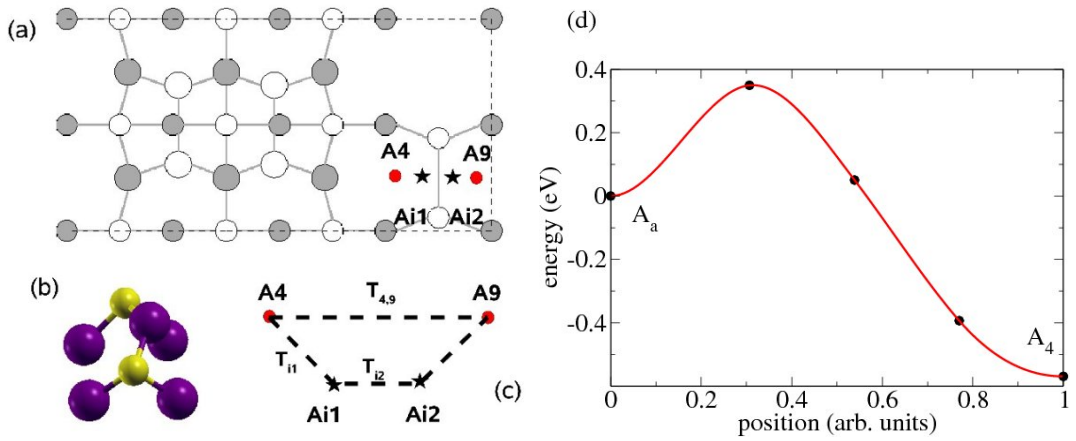

FIG. 10: (Color online) Additional adsorption sites A_{i1} and A_{i2} due to In insertion into the As in-dimer on the β_2 surface reconstruction. (a) The locations of the adsorption sites are indicated by stars. (b) Atomic configuration. (c) Scheme of the transitions between the A_{i1} and A_{i2} adsorption sites and the neighboring sites. (d) Energy profile for barrier T_{i1} from the besides in-dimer adsorption site A_4 to A_{i2}.

B. 1.75 ML InAs on GaAs $(001)\beta_2(2\times4)$ vs InAs $(001)\beta_2(2\times4)$

In this subsection we compare our results for In adsorption on the $\beta_2(2\times4)$ reconstruction of the InAs WL on GaAs(001) with the results for In adsorption on the $\beta_2(2\times4)$ reconstruction of pure InAs(001) of ref. [21, 22]. The main difference between the two cases is that the InAs WL on GaAs is subjected to a compressive strain on the (001) plane. Thus, the comparison allows us to evaluate the effect of the WL strain on In adsorption. We principally refer to Fig.2 of ref.[21] and to Table VI of the present paper, where we have reported the energies of the minima of In on the InAs surface [33].

In the case of pure InAs[21], only six minima were calculated and their positions on the surface are almost the same as those calculated by us. In particular, only one minimum B_8 in the *bridge in-dimer* position (see Fig. 11) was found halfway between the two equal minima A_6 and A_8 calculated by us for the InAs/GaAs case. The two minima A_6 and A_8 are separated by a relatively high barrier of 300 meV in our calculation. We recall here that for α_2 we calculate barriers only 42 and 142 meV high between the same adsorption sites. (A_6 and A_8 are no more equivalent in α_2).

In the case of pure InAs, the *besides in-dimer* B_4 and B_9 show the strongest binding. In

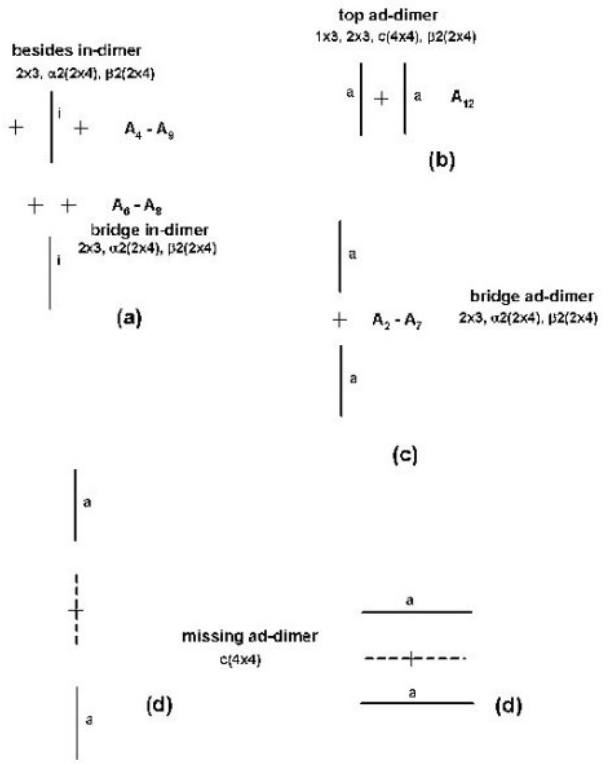

FIG. 11: Scheme of the main adsorption sites for an In adatom on (001) reconstructed III-V surfaces: (a) besides in-dimer and bridge in-dimer locations, (b) top ad-dimer location, (c) bridge ad-dimer location, and (d) missing ad-dimer locations.

the case of the InAs WL on GaAs, instead, the more strongly bonded sites are located at the *bridge in-dimer* positions A_6 and A_8. From Tables III and VI we see that the energy difference between the sites (4-9) and (6-8) is larger for the InAs WL on GaAs case (240 meV vs 61 meV). It is reasonable to think that this difference is to be ascribed to the strain originated by the lattice mismatch between InAs and GaAs. Also the absence of the shallow adsorption sites corresponding to A_1, A_5, A_3 and A_{10} could be originated by the absence of the strain.

Nevertheless, it is possible that these differences are originated also by the different grid resolution used for calculating the PES, or by the interpolation algorithms that sometimes are not able to identify correctly the minima or by the difference between GGA used in ref. [21] and LDA used in this work.

C. In on InAs/GaAs $\beta_2(2\times4)$ vs Ga on GaAs $\beta_2(2\times4)$

At this stage of the discussion we compare our results for the β_2 reconstruction with the results obtained in ref. [20], where the PES of a Ga adatom on the $\beta_2(2\times4)$ surface reconstruction of GaAs(001) was studied. This comparison evidences the different behavior of In and Ga adsorbates, as opposed to the WL composition.

In the case of Ga on GaAs(001) only three minima were reported (without considering the additional minima where Ga breaks the dimers). Two minima are at *bridge ad-dimer* positions while the third one is at a *bridge in-dimer* position. These adsorption sites correspond to the A_2, A_7 and A_6-A_8 minima on the InAs WL and to B_2, B_7 and B_8 minima of the In on InAs(001) case [21]. These minima are quite stable. Notice the missing of the A_{12} adsorption site on the *top ad-dimer* location, which is present in the case of the In adsorbate on β_2 reconstructed InAs covered surfaces. Also the adsorption sites in the *besides in-dimer* locations are missing in this case.

D. In adatom on InGaAs surfaces

In this section we compare with the results of ref. [12, 16] where InGaAs reconstructions of the WL on GaAs were considered. The PESs of the In adatom on: (i) $In_{2/3}Ga_{1/3}As(001)$ (2×3) (corresponding to a In coverage $\theta=0.66$), (ii) $In_{2/3}Ga_{1/3}As(001)$ (1×3) (corresponding to $\theta=0.66$), and (iii) GaAs(001) $c(4\times4)$ (corresponding to $\theta=0$) surface reconstructions were studied. From all these calculations we can see that one adsorption site is always located in a *top ad-dimer* position, in the same configuration of the A_{12} adsorption site on β_2 of this work. The depth of these adsorption sites defined by the height of the lowest barrier confining the adsorbate are: 140 meV, 60 meV, 100 meV, 385 meV and 135 meV for (2×3), (1×3), $c(4\times4)$, InAs $\beta_2(2\times4)$ and InAs WL on GaAs $\beta_2(2\times4)$, respectively. We can see that these minima are not strongly bonded, apart from the case of In on pure InAs(001) β_2 reconstructed surface.

The deepest minima are located at the *besides in-dimer* location, both in the case of the (2×3) reconstruction of [12] and of the reconstructions studied in this work. In the case of the $c(4\times4)$ reconstruction, stable locations are at the *missing ad-dimer* sites (see fig. 11). In these adsorption sites the In adatom binds to four As atoms below. In the case of

the (1×3) reconstruction the stable location sees the In atoms bonded to the cations layer below.

V. CONCLUSIONS

We have carried out a first-principles study of the adsorption properties of an In adatom deposited on a InAs wetting layer on GaAs(001) reconstructed $\alpha_2(2 \times 4)$ or $\beta_2(2 \times 4)$. We have first studied the equilibrium geometry of the surfaces and the relative phase stability with respect to the growth conditions. We have found that, in the case of the InAs WL the interlayer distances are systematically higher than those of pure GaAs, owing to the compressive strain. Moreover, we have found that the α_2 reconstruction of the InAs WL is favored over the β_2 reconstruction, for a wider range of growth conditions, when compared to the bare GaAs(001) surface.

We have analyzed the PES for an In adatom determining the adsorption sites and the saddle points for both α_2 and β_2 reconstructions. We have found 11 minima in the PES for both reconstructions. Most of them occur in the same positions in both cases. Two minima are instead specific of the α_2 and β_2 reconstructions, due to the presence on β_2 of an additional As ad-dimer. For the adsorption sites present on both reconstructions, we have studied the change of the adsorption energy and location caused by the presence or absence of the second As ad-dimer. We have identified two low-energy trenches along the $[\bar{1}10]$ direction, alongside the in-dimer chain, for both α_2 and β_2.

The comparison to analogous studies reported in the literature has revealed some general features for the In adsorption on different surface reconstructions. In particular, we have found that stable adsorption sites are always located: (i) besides the in-dimers, (ii) at the bridge positions between in-dimers, (iii) between ad-dimers (only for β_2 which has two adjacent As ad-dimers), and (iv) at the bridge between ad-dimer positions. We have identified also other shallower adsorption sites which are more reconstruction specific and are related to α_2 having a lower symmetry than β_2.

site	energy (meV)
A_1	220
A_2	387
A_3	312
A_4	49
A_5	344
A_6	99
A_7	559
A_8	0
A_9	112
A_{10}	868
A_{11}	498
A_i	-100
A_a	239

TABLE I: Adsorption energies for the In adatom in the different adsorption sites of the α_2 surface reconstruction, relative to the A_8 energy, labeled as A_n. The labels A_i and A_a refer to the configurations of the adsorbate into the in-dimer and the ad-dimer, respectively.

Acknowledgments

The authors would like to thank A. Ishii for providing us with the data about In adsorption on InAs [21]. We acknowledge the support of the MIUR PRIN-2005, Italy. The calculations were performed at CINECA-Bologna under the grant "Iniziativa Calcolo Parallelo del CNR-INFM", and at LabCsai in Modena.

APPENDIX A: ENERGIES OF MINIMA AND SADDLE POINTS

In this appendix we report all the numerical values calculated for minima and saddle point energies.

saddle	energy (meV)
$T_{2,9}$	895
$T_{2,7}$	676
$T_{3,7}$	635
$T_{3,4}$	456
$T_{4,9}$	498
$T_{4,5}$	453
$T_{1,10}$	893
$T_{6,8}$	142
$T_{8,9}$	428
$T_{1,9}$	272
$T_{1,8}$	418
$T_{5,11}$	554
$T_{10,11}$	929
$T_{7,11}$	743
$T_{11,7}$	750
T_{i1}	613
T_{i2}	493
T_{a1}	893
T_{a2}	926
T_{a3}	1117

TABLE II: Energies of the saddle points in the PES of the α_2 surface reconstruction, relative to the A_8 adsorption energy. The saddle points connecting the minima A_n and A_m are labeled by $T_{n,m}$, while the labels T_{in} (T_{an}) indicate the saddle points between the minima into the in-dimer (ad-dimer) and the neighboring sites, as shown in Fig. 8 (Fig. 7)

site	energy (meV)
A_1, A_5	216
A_2, A_7	506
A_3, $A_{3'}$	323
A_4, A_9	240
A_6, A_8	0
A_{12}	588
A_i	-330
A_a	158

TABLE III: Adsorption energies for the In adatom in the different adsorption sites of the β_2 surface reconstruction, relative to the A_8 energy, labeled as A_n. The labels A_i and A_a refer to the configuration of the adsorbate into the in-dimer and the ad-dimer, respectively.

site	ΔE (meV)	$\Delta r/a_0$
A_1	-134	0.022
A_2	-7	0.069
A_3	-121	0.330
A_4	66	0.168
A_5	-259	0.350
A_6	-224	0.100
A_7	-179	0.588
A_8	-125	0.018
A_9	4	0.031

TABLE IV: Adsorption energy differences and position displacements between the In adsorbate for the corresponding adsorption sites of the β_2 and the α_2 reconstructions.

saddle	energy (meV)
$T_{4,5}$	392
$T_{5,6}$	424
$T_{1,12}$	976
$T_{12,2}$	723
$T_{2,11}$	727
$T_{2,3'}$	974
$T_{2,7}$	589
$T_{6,3}$	577
$T_{4,3}$	424
$T_{4,9}$	701
$T_{6,8}$	296
T_{i1}	589
T_{i2}	94
T_{a1}	760
T_{a2}	610
T_{a3}	1024

TABLE V: Energies of the saddle points in the PES of the β_2 surface reconstruction, relative to the A_8 (β_2) adsorption energy. The saddle points connecting the minima A_n and A_m are labeled by $T_{n,m}$, while the labels T_{in} (T_{an}) refer to the saddle points between the minima into the in-dimer (ad-dimer) and the neighboring sites, as shown in Fig. 10 (Fig. 9).

site	energy (meV)
B_2, B_7	302
B_4, B_9	0
B_8	61
B_{11}	163

TABLE VI: Adsorption energies (calculated with respect to B_4 energy) for the In adatom in the different adsorption sites on the InAs β_2 surface reconstruction, labeled as B_n (see ref. [21, 33]). The positions of the minima B_n corresponds to the minima A_n in fig. 5(b).

[1] I. N. Stranski, and L.Karstanov, Sitzungsber. Akad. Wiss. Wien, Math Naturwiss. Kl. IIb **146**, 797 (1938).

[2] C. Ratsch, Phys. Rev. B **63**, 161306(R) (2001)

[3] P. Kratzer, E. Penev, and M. Scheffler, Appl. Surf. Sci. **216**, 436 (2003)

[4] E. Penev and P. Kratzer, "First-Principles study of InAs/GaAs(001) heteroepitaxy", in: *B.A. Joyce et al. (eds.) Quantum Dots: Fundamentals, Applications and Frontiers*, NATO Science Series II, Vol. **190**, p 27-42, (Springer Verlag, Berlin) (2005).

[5] F. Patella, F. Arciprete, E. Placidi, S. Nufris, M. Fanfoni, A. Sgarlata, D. Schiumarini, and A. Balzarotti Appl. Phys. Lett. **81**, 2270 (2002).

[6] N. Grandjean, and J. Massies, J. Crystal Growth **134**, 51 (1993)

[7] P.A. Bone, J.M. Ripalda, G.R. Bell, and T.S. Jones, Surf. Sci. **600**, 973 (2006).

[8] J.G. Belk, C.F. McConville, J.L. Sudijono, T.S. Jones, and B.A. Joyce, Surf. Sci. **387**, 213 (1997).

[9] F. Patella, F. Arciprete, M. Fanfoni, and A. Balzarotti, Appl. Phys. Lett. **88**, 161903 (2006)

[10] P. Kratzer, C. G. Morgan, and M. Scheffler Phys. Rev. B **59**, 15246 (1999)

[11] E. Penev, " On the theory of surface diffusion in InAs/GaAs(001) heteroepitaxy", Ph.D thesis, Technische Universität Berlin (2002)

[12] E. Penev, S. Stojković, P. Kratzer, and M. Scheffler, Phys. Rev. B **69**, 115335 (2004)

[13] W. Kohn, and L. J. Sham Phys. Rev **140**, A1133 (1965).

[14] D. M. Ceperley, and B. J. Alder, Phys. Rev. Lett. **45**, 566 (1980)

[15] J. P. Perdew, and A. Zunger, Phys. Rev. B **23**, 5048 (1981)

[16] E. Penev, P. Kratzer, and M. Scheffler, Phys. Rev. B **64**, 085401 (2001)

[17] W. G. Schmidt, F. Bechstedt, N. Esser, M. Pristovsek, Ch. Schultz, and W. Richter, Phys. Rev. B **57**, 14596 (1998)

[18] L. Wang, P. Kratzer, and M. Scheffler, Jpn. J. Appl. Phys. **39**, 4298 (2000)

[19] J. G. LePage, M. Alouani, D. L. Dorsey, J. W. Wilkins, and P. E. Blöchl, Phys. Rev. B **58**, 1499 (1998)

[20] A. Kley, P. Ruggerone, and M. Scheffler, Phys. Rev. Lett **79**, 5278 (1997)

[21] K. Fujiwara, A. Ishii, and T. Aisaka, Thin Sol. Films **464-465**, 35 (2004)

[22] A. Ishii, K. Fujiwara, and T. Aisaka, Appl. Surf. Sci. **216**, 578 (2003)

[23] A. Kley, "Theoretische Untersuchungen zur Adatomdiffusion auf niederindizierten Oberflächen von GaAs", Ph.D. Thesis, Technische Univ. Berlin (1997).

[24] C. Stampfl, and C. G. Van de Walle Phys. Rev. B **59**, 5521 (1999)

[25] P. Kratzer, C.G. Morgan, and M. Scheffler, Prog. Surf. Sci. **59**, 135 (1998)

[26] P. Pechukas, *Dynamics of molecular collisions*, Part B (W. H. Miller ed.), Plenum Press, New York (1976).

[27] D. G. Truhlar, W. L. Hase, and J. T. Hynes, J. Phys. Chem. **87**, 2664 (1983).

[28] D. G. Truhlar, B. C. Garret, and S. J. Klipenstein, J. Phys. Chem. **100**, 12771 (1996).

[29] H. Jónsson, G. Mills, and K. W. Jacobsen, in: B. J. Berne, G. Ciccotti, D. F. Cocker (Eds.) *Classical and quantum dynamics in condensed phase simulations* World scientific (1998)

[30] G. Mills, and H. Jónsson, Phys Rev. Lett. **72**, 1124 (1994)

[31] pwscf website: http://www.pwscf.org

[32] N. Moll, A. Kley, E. Pehlke, and M. Scheffler, Phys. Rev. B **54** 8844 (1996)

[33] A. Ishii, private communication